Real-Time Battery Thermal Management for Electric Vehicles

Eugene Kim and Kang G. Shin
Department of Electrical Engineering and Computer Science
The University of Michigan, Ann Arbor, MI 48109-2121, U.S.A.
{kimsun, kgshin}@umich.edu

Jinkyu Lee
Department of Computer Science and Engineering
Sungkyunkwan University, Suwon, Gyeonggi-Do, Republic of Korea
jinkyu.lee@skku.edu

ABSTRACT

Electric vehicles (EVs) are powered by a large number of battery cells, requiring an effective battery management system (BMS) to maintain the battery cells in an operational condition while providing the necessary power efficiently. Temperature is one of the most important factors for battery operation, and existing BMSes have thus employed simple thermal management policies so as to prevent battery cells from very high and low temperatures which may likely cause their explosion and malfunction, respectively. In this paper, we study thermo-physical characteristics of battery cells, and design a battery thermal management system that achieves efficiency and reliability by *active thermal controls*.

We first analyze the effect of a temperature change on the basic operation of a battery cell. We then show how it can cause thermal and general problems, e.g., a thermal runaway that results in explosion of battery cells, and unbalanced state of charge (SoC) that degrades battery cells' performance. Based on this understanding of thermal behavior, we finally develop temperature-control approaches which are then used to design a battery thermal management system. Our simulation results demonstrate that the proposed thermal management system improves battery performance by up to 58.4% without compromising reliability over the existing simple thermal management.

Categories and Subject Descriptors

C.3 [**Special-Purpose and Application-Based Systems**]: Real-time and embedded systems; I.6.3 [**Simulation and Modeling**]: Applications

1. INTRODUCTION

While electric vehicles (EVs) become popular for their environmental friendliness and low fuel cost, they have not fully replaced internal combustion engine vehicles due to the risk of explosion of battery cells, the high price for the large number of battery cells required, and the limited availability of charging stations. As many researchers pointed out [1, 4, 14, 23], temperature is one of the most critical factors in designing and operating EVs. For example, an extremely high temperature may lead to explosion or performance degradation of battery cells. In contrast, a battery system operating at a very low temperature might be dysfunctional or have a low capacity due to low reaction rates with freezing electrolytes. In addition, the discharge rate of cells varies with temperature, altering their capacity.

To address the challenges related to temperature, most automotive manufacturers have developed their own thermal management systems for their EVs [9, 10]. That is, a BMS (Battery Management System) monitors the temperature of battery cells, and triggers the thermal control when temperature deviates from the normal operational range. This control includes both cooling and heating, and existing controls are all or nothing—whether or not they cool/heat *all* the battery cells connected in parallel. However, such coarse-grained controls result in a large safety margin and hence inefficiency. More importantly, they do not exploit temperature for more efficient management, in that more sophisticated controls of temperature even within the normal operational range may yield better battery performance.

The goal of this paper is to develop thermal management for an efficient and reliable BMS. Efficiency is defined by "the ratio of the useful energy delivered by a dynamic system to the energy supplied to it" [26]; we

achieve efficiency by maximizing *operation-time* [18], or the cumulative time for a BMS to provide the required power after a full charge. We achieve reliability by guaranteeing that a BMS provides the required power throughout the given battery warranty period without an explosion or malfunction, while letting its cells undergo charge-and-discharge cycles.

To improve efficiency without compromising reliability, we need a *cyber-physical perspective* of battery thermal management, integrating and coordinating between cyber and physical parts. For physical parts, we should understand thermo-physical characteristics of battery cells and external thermal stress conditions, as they have significant impact on battery performance. By carefully accounting for these non-linear physical properties and abstracting the characteristics in the cyber space as shown in Fig. 1, we can develop desirable thermal management that reduces the safety margin, thereby increasing the efficiency of the entire battery system in EVs.

To achieve this goal, we use temperature as a control knob; beyond a simple temperature control only for the normal operational range, we design a battery thermal management system, which actively controls temperature for more efficient and reliable operations. This requires understanding the thermal and general issues of batteries that affect the efficiency and reliability. Therefore, we analyze the issues based on battery thermo-physical characteristics and their impact on the electrical state of battery cells. Based on this analysis, we derive strategies in achieving the goal, and then propose a battery thermal management system with cell-level thermal controls. Our policy boosts the performance of cells temporarily when high power is required, while resting cells otherwise to reduce stresses; we will present details of our policy along with their underlying principles. To evaluate the proposed BMS, we adopt realistic workloads based on real driving patterns, and simulate them with a widely-used battery simulator. Our simulation results demonstrate the effectiveness of the proposed battery thermal management, improving the operation-time up to 58.4%, without sacrificing reliability, over the existing BMS.

This paper makes the following three main contributions:

- Abstraction of thermo-physical characteristics in the cyber-space to address the issues associated with efficient and reliable thermal management;
- Design of a battery thermal management system with a new architecture, which is, to our best knowledge, the first comprehensive study to exploit temperature as a control knob for BMSes; and
- In-depth evaluation of the proposed thermal management, demonstrating its significant improvement of efficiency without compromising reliability.

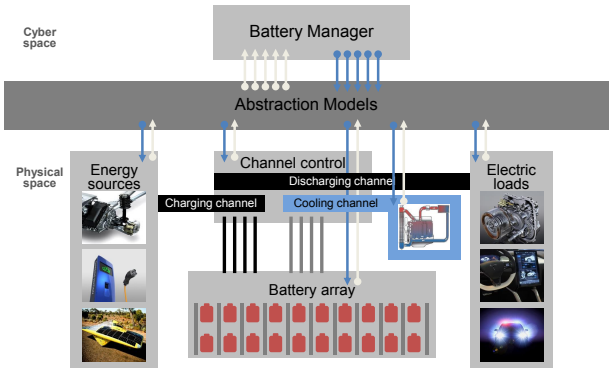

Figure 1: Cyber-physical perspective for a BMS

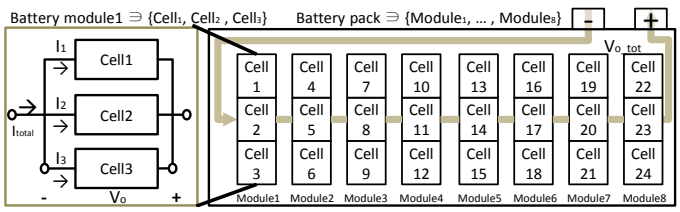

Figure 2: A battery pack with modules and cells

The paper is organized as follows. Section 2 presents general and thermal management approaches in existing BMSes, and Section 3 formally states the problem we want to solve via thermal management. Section 4 describes physical characteristics related to thermal and general issues of large-scale battery systems, and Section 5 presents our battery thermal management system. Section 6 evaluates our system via realistic simulations, and finally, Section 7 concludes the paper.

2. BACKGROUND

As illustrated in Fig. 2, a battery pack consists of some interfaces (e.g., electrodes) and several battery modules, each of which is composed of several battery cells. In a battery module, all the battery cells are connected in parallel, reducing the possibility of battery failure caused by a cell-level failure. The modules in a pack are usually connected in series, enabling the battery pack to provide a high voltage and power.

A BMS is responsible for powering EVs while protecting hundreds/thousands of battery cells from damage and keeping them in an operational condition. For a BMS to perform these functions, battery cells should be properly controlled because their safety and performance depend on stress conditions around them. In this section, we discuss the battery properties and the related work thereof.

2.1 Battery Scheduling for Efficient Battery Management

Rate-capacity and recovery effects are the most prominent physical properties for efficient battery management. The rate-capacity effect means that the higher the discharge rate, the lower the deliverable capacity. The recovery effect means that a rest restores the output voltage temporarily dropped by large discharge current. Therefore, we can increase the capacity of batteries, by minimizing the discharge rate per cell and resting battery cells.

State-of-Charge (SoC) represents percentage of deliverable charge, from 0% with no charge, to 100% with full, and balancing SoC is one of the most critical issues affecting the performance of large-scale battery systems because the performance of a large battery pack depends on the electrical state of the most worn battery cell in the pack.

To achieve better battery performance, a line of work has focused on *battery scheduling* that equalizes SoC and/or reduces the discharge rate [2, 11, 12, 17, 18]. They control switches to draw energy from battery cells at a proper discharge rate. For example, when an electric motor needs high power, a battery manager connects all the cells to the electric load to improve battery efficiency. In contrast, when the motor demands low power from the battery, the battery manager disconnects some cells with low SoC, achieving recovery of the output voltage and equalization of SoC.

2.2 Thermal Management of Large-scale Batteries

Besides discharge behaviors and SoC balancing, battery thermal characteristics are also important to their efficiency, operation and safety. Of many characteristics, we will focus on the following two major characteristics. First, battery efficiency improves temporarily at "instant high temperature" due to the increased chemical reaction rate and ion mobility. However, the "cumulative exposure to high temperature" causes the permanent lifetime to decline because of its acceleration of irreversible side reaction. Therefore, most BMSes are required to restrict each cell within a certain temperature range to achieve reasonable performance. Every EV must thus be equipped with a thermal management system that keeps cell temperature within the operational range, requiring both cooling and heating. Whenever the temperature of a battery pack deviates from an operational temperature range, thermal management is activated to guarantee thermal stability of batteries [9, 10, 16, 28, 29].

For cooling, the radiator transfers heat from the fluid inside to the air outside, thereby cooling the fluid, which in turn cools batteries. Heating is also required for driving at extremely cold temperature. For example, GM Chevy Volt [10] uses 144 thermal fins to actively cool/heat 288 battery cells with a coolant flow valve controlling cooled/heated coolant flows. Ford Focus [9] is also equipped with an active liquid-cooling and heating system for thermal management of its lithium-ion battery packs.

So far, this simple approach has been effective for the normal operation of battery cells during a vehicle warranty period; a warranty can be made by thoroughly testing battery cells' performance in thermal experiment chambers. However, such a passive, coarse-grained thermal control does not take full advantage of thermal management systems. By understanding battery thermal characteristics and controlling temperature, we can improve battery's capacity without compromising the lifetime of battery cells. This is because heating the cell increases the battery performance instantaneously, while cooling the cell for the situation of requiring low power can delay the drop of lifetime. To regulate cell temperature systematically, we analyze battery dynamics and propose active and cell-level thermal management for more efficient and reliable BMSes.

3. PROBLEM STATEMENT

In this paper, we would like to develop "good" thermal management for more efficient and reliable battery systems. For this, we state the problem of thermal management for which we first introduce relevant terms.

A battery pack in EVs supplies DC power to an inverter which operates the electric motors in EVs. To operate motors, a power inverter needs an applicable input voltage (V_{app}) during the vehicle's operation. Then, the *operation-time* (ℓ_{op}) is defined as the cumulative time for a battery pack to provide the required power with applicable output voltage range after a full charge [18].

Therefore, a BMS should enable its battery pack to supply the required power ($P_{req}(t)$) to electric motors while maintaining output voltage no less than the applicable input voltage for a long operation-time. Meanwhile, the operation-time should be kept long during the battery warranty period; otherwise, the vehicle requires a larger battery pack and/or batteries must be recharged more frequently.

In this paper, we want to develop a BMS that yields a long operation-time during the warranty period by controlling the temperature of battery cells. We can control battery temperature by selecting the coolant type in each thermal fin at each time instant to be cooled or heated, which will be detailed in Section 5.3. That is, the coolant type is used as a control knob for our BMS. Our goal is then to determine the coolant type at each time instant ($C_{fin}(t)$) such that the operation-time (ℓ_{op}) is maximized during the warranty period without any malfunction or explosion, which is formally expressed as:

Given stress conditions $\{P_{req}(t), T_{ext}(t)\}_{0<t<t_{warr}}$, determine $\{C_{fin}(t)\}_{0<t<t_{warr}}$, such that ℓ_{op} is maximized

at t_{warr} without any malfunction or explosion in $[0, t_{warr}]$, where $T_{ext}(t)$ is temperature outside the battery pack, and 0 and t_{warr} are the time at the beginning and end of the battery warranty period, respectively. Note that the stress conditions and the control of $C_{fin}(t)$ are valid/necessary only during operation of the EV in $[0, t_{warr}]$.

Note that ℓ_{op} monotonically decreases over time, because the performance of a battery keeps on degrading over time and never recovering. Therefore, ℓ_{op} at any time during the warranty is at least as much as that at t_{warr}.

4. ABSTRACTION OF PHYSICAL DYNAMICS OF BATTERIES

Several battery dynamics under stress conditions affect the performance and safety of battery systems. For example, uncontrolled high temperature may cause explosion, while an extremely low temperature reduces the battery's performance, potentially leading to failure to power the electric vehicle. Therefore, the impacts and dependencies of control knobs and external conditions on battery dynamics should be analyzed to improve the safety and performance of a battery system.

To this end, we will first identify the factors that affect the performance by bridging different abstraction models for battery physical dynamics. Then, based on the unified abstraction model, we will address how a change in temperature affects battery physical dynamics, which will be a basis for our battery thermal management to be described in Section 5.

4.1 Abstraction of Battery Characteristics

By analyzing the dependency on thermal conditions and the impacts on states of batteries, we can figure out how controllable thermal conditions affect the output voltage of the entire battery system and each cell's temperature.

4.1.1 *Circuit-Based Battery Model ($V_o = f(R_{int}, I_d, SoC)$)*

Output voltage (V_o) dictates the operation-time of a battery system, and the output voltage is greatly affected by battery cells' internal states. A circuit-based battery model uses fundamental electric elements, such as internal resistance (R_{int}), discharge current (I_d), and open-circuit voltage (V_{oc}) to represent the cell's internal states, and explains the output voltage by basic circuit theory as described in Fig. 3 and Eq. (1).

When the cell is connected to an external load, an electron flow (I_d) occurs from the anode to the cathode through the external load. Open-circuit voltage (V_{oc}) is the difference of electrical potential between two terminals of the cell when disconnected from any circuit, and it largely depends on deliverable charges (SoC) in battery cells. The internal resistance (R_{int}) represents all

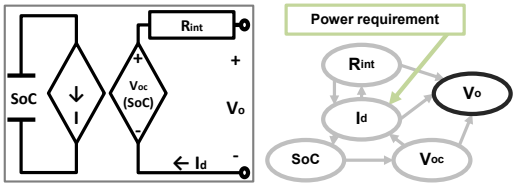

Figure 3: Circuit-based battery model

the factors causing voltage drop between open-circuit voltage (V_{oc}) and output voltage (V_o) when the power source delivers current. In addition, large capacitors are adopted to represent states of deliverable charge (SoC) of cells. Then, the output voltage is expressed as [23]:

$$V_o = V_{oc} - I_d R_{int} = f(SoC) - I_d R_{int}, \qquad (1)$$

which says that a change in internal resistance affects output voltage as follows:

P1. Internal resistance ⇒ Output voltage ($R \uparrow \rightarrow V_o \downarrow$): As the internal resistance gets higher, the output voltage decreases.

Supplying the required power (P_{req}) to the electric load induces power dissipation (P_d) in a battery pack. That is, total power consumption (P_{bat}) in a battery pack (P_{bat}) consists of the two power consumption parameters (P_{req} and P_d) as shown in the following equation [23]:

$$\begin{aligned} V_{oc} = V_o + I_d R_{int} \quad &\Rightarrow \quad V_{oc} I_d = V_o I_d + I_d^2 R_{int} \\ &\Rightarrow \quad P_{bat} = P_{req} + P_d. \end{aligned} \qquad (2)$$

Therefore, to use batteries efficiently and increase the operation-time of a battery pack, a BMS should reduce power dissipation (P_d) during operation, which is recorded as follows.

P2. Internal resistance ⇒ Power dissipation ($R \uparrow \rightarrow P_d \uparrow$): As internal resistance gets higher, power dissipation increases.

Since the output voltages of the cells connected in parallel should be the same and the variation of open-circuit voltage is small, discharge current depends on internal resistance according to Eq. (1). Then, the discharge current of a cell with larger internal resistance is lower than that of the other cells in the module, as recorded in the following statement:

P3. Internal resistance ⇒ Discharge rate ($R \uparrow \rightarrow I_d \downarrow$): As internal resistance gets higher, the discharge rate per cell decreases in a module.

4.1.2 *Relation between Internal Resistance and Cell Temperature ($R_{int} = f(T_{cell}, t)$)*

As shown in P1 and P2, internal resistance is an important parameter that affects batteries' performance.

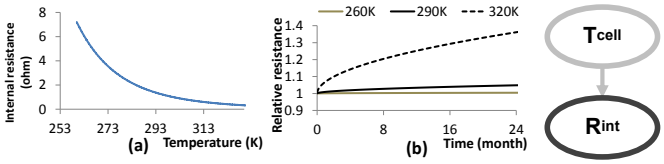

Figure 4: Internal resistance increases as temperature decreases, and relative internal resistance increases as time to expose to high temperature increases; both graphs are obtained with evaluation tools/settings to be described in Section 6.

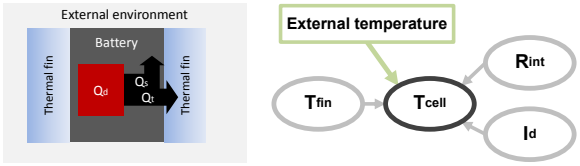

Figure 5: Battery thermal dynamics

Therefore, we describe how internal resistance varies with thermal stresses during operation.

Before presenting the effect of temperature on internal resistance, we define two terms related to time interval. An *operation cycle* represents a cycle of a battery cell's operation from its full charge to no charge. A *calendar life* is a duration from a battery cell's production to its warranty period (e.g., 5 years). We describe how temperature affects internal resistance, when a given temperature lasts during (i) an operation cycle, and (ii) a calendar life.

Regarding (i), a higher temperature stimulates the mobility of electron or ion, temporarily reducing the cell's internal resistance and increasing its capacity (by P2). For example, as shown in Fig. 4(a), resistance with 320K is smaller than that with 290K. Therefore, during an operation cycle, the following relation holds:

P4. Temperature ⇒ Internal resistance ($T\uparrow \rightarrow R\downarrow$ (operation cycle)): As temperature during an operation cycle increases, internal resistance decreases.

In literature, relation between internal resistance and cell temperature is well-described by a polynomial model, and experimental results substantiate its effectiveness [27]:

$$R_{int} = c_3 T_{cell}^3 + c_2 T_{cell}^2 + c_1 T_{cell} + c_0. \quad (3)$$

This model dictates cell temperature (T_{cell}) for the required internal resistance (R_{int}).

On the other hand, a long-term temperature exposure affects internal resistance the other way around, as explained next. Battery performance deteriorates over time, regardless of whether the battery is used or not, which is known as "calendar fade", and it can be represented by a rise of internal resistance as shown in Fig. 4(b). There are two key factors influencing the calendar life, namely temperature (T) and time (t), and empirical evidences show that these effects can be represented by two relatively simple mathematical dependencies (t and T). The extent of deterioration can be assessed by relative resistance (μ), which is expressed as [33, 34]:

$$\mu(T;t) = 1 + exp(\beta_0 + \beta_1 \cdot \frac{1}{T}) \cdot t^{\rho}, \quad (4)$$

where β_0, β_1, and ρ represent the model parameters. According to Eq. (4), the following statement holds:

P5. Temperature over time ⇒ Resistance ($t\uparrow, T\uparrow \rightarrow R\uparrow$ (calendar life)): As time to high temperature exposure increases during a calendar life, internal resistance increases.

4.1.3 *Thermal Behavior Model* ($T_{cell} = f(T_{amb}, R_{int}, I_d)$)

While internal resistance depends on cell temperature (P4 and P5), cell temperature, in turn, varies with a battery internal state and external stress.

Any battery operation generates heat due to internal resistance when the cell delivers power to electric loads, which is also known as *joule heating* ($I_d^2 R_{int}$ loss). Some part of generated heat (Q_d) would be released on the surface of cells (Q_t), and the remaining heat is absorbed into cell materials (Q_s), which can be calculated by [3]:

$$Q_d = I_d^2 R_{int}, Q_s = C_{cell} \frac{dT_{cell}}{dt},$$
$$Q_t = Ah(T_{cell} - T_{amb}),$$

where A is the surface area, h the heat transfer coefficient, T_{amb} temperature around the cell, and C_{cell} heat capacity, respectively. Note that ambient temperature (T_{amb}) is affected by external temperature (T_{ext}) and temperature of thermal fins (T_{fin}).

Eq. (5) shows Bernardi's energy balance [3], and it can explain cell temperature (T_{cell}) variation by heat generation (Q_d) as shown in Fig. 5. Then, Eq. (5) can be solved by Eq. (6) as follows.

$$Q_d = Q_t + Q_s, \quad (5)$$

$$T_{cell}(t+\Delta t) = T_{cell}(t) + \Delta t[c_1(T_{cell} - T_{amb}) + c_0 I_d^2 R_{int}], \quad (6)$$

where t is the current time and Δt the time interval. Based on the equation, the following statement holds.

P6. Discharge current ⇒ Heat generation ($I_d\uparrow \rightarrow T\uparrow$): As discharge current increases, heat generation increases.

If we bridge all the battery characteristics discussed in P1–P6, we have an abstract layer from the temperature

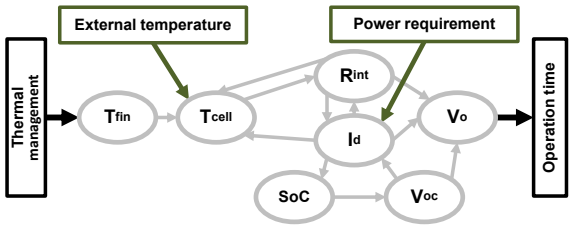

Figure 6: Abstraction of battery dynamics

of thermal fins (T_{fin}) to operation-time, as described in Fig. 6.

4.2 Battery Physical Dynamics According to a Thermal Change

Our goal is to develop thermal management so as to increase battery operation-time during its warranty period without explosion and malfunction. To figure out battery dynamics affecting the operation-time and safety, we constructed an abstraction layer by accumulating several physical dependencies as shown in Fig. 6. We revisit the physical dependencies (P1–P6) on the abstraction to analyze the battery physical dynamics, which will be a basis for our thermal management to be presented in Section 5.

4.2.1 Thermal runaway (P3, P4 and P6)

Thermal runaway is one of the most serious thermal issues affecting safety of a battery cell, and results in extremely high temperature and current. A rise in the temperature of a battery cell decreases its internal resistance (by P4) and increases its current (by P3) in a parallel connection, which, in turn, raises its temperature (by P6); this process may repeat, as illustrated in Fig. 7. Since extremely high temperature (above around $80°C$) may cause an explosion due to decomposition of materials [23, 14], the thermal stability of battery cells should be maintained.

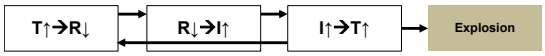

Figure 7: Increase in temperature of a cell causes a further increase in the temperature, potentially resulting in explosions of the battery cells because of material decomposition inside the cells.

4.2.2 Malfunction at low temperature (P1 and P4)

Each BMS has a specification of applicable output voltage (V_{app}). The BMS should guarantee delivery of the required power within V_{app} range. However, a decrease in temperature increases internal resistance (by P4), and it may cause a higher voltage drop (by P1) in order to supply the same current. Output voltage (V_o) drops below the applicable voltage (V_{app}) making a power inverter unable to operate in a specified condition, and hence failing to provide the required power to the vehicle's electric motors. Fig. 8 illustrates how a low temperature causes malfunction.

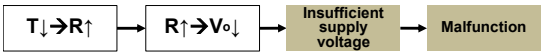

Figure 8: Low temperature leads to high internal resistance and voltage drop.

4.2.3 Short operation-time at lower temperature (P2 and P4)

A decrease in temperature reduces the mobility of charges and chemical reaction in cells, which can be represented by the increased internal resistance (by P4). This increased internal resistance implies a larger power dissipation during operation (by P2), which reduces operation-time as shown in Fig. 9. For example, it is reported that a drop of just 20 Celsius degrees can drain 10 – 20% of a battery's charge [8].

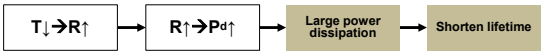

Figure 9: Low temperature leads to higher internal resistance and power dissipation.

4.2.4 Performance degradation due to continuous exposure to high temperature (P1, P2 and P5)

Operating under continuous exposure to high temperature induces a rapid increase in internal resistance (by P5) due to the acceleration of irreversible side reactions [23]. The increase in internal resistance causes energy dissipation of cells, shortening their operation-time. Faster performance degradation may also cause battery malfunction even during its warranty period (by P1 and P2), potentially leading to tragic accidents or financial loss. Figs. 8 and 9 illustrate what we explained so far.

4.2.5 Unbalanced SoC (P4, P5 and P3)

Uneven temperature distribution causes different resistances between battery cells in a battery pack (by P4 and P5). Since the discharge rate depends on internal resistance (by P3), the discharge rates available for different cells are uneven, leading to unbalanced SoC among the cells in a battery pack as shown in Fig. 10.

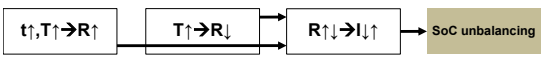

Figure 10: Uneven degradation and temperature of cells cause different internal resistances of battery cells, leading to different discharge current and SoCes.

4.2.6 *Rate-capacity effect and recovery effect (P4, P5, P3 and P6)*

A higher discharge rate causes more capacity loss yielding larger voltage drop due to heat loss (by P5), called *rate-capacity effect* explained in Section 2.1. In case of a very low (or zero) discharge rate, the battery can recover its capacity loss to some extent during high-rate of discharge, called *recovery effect*, also discussed in Section 2.1. Uneven temperature distribution may cause more unexpected discharge current (by P3, P4, P5), leading to more rate-capacity effect in some cells as shown in Fig. 11. Also, uneven discharge rates cause different amounts of heat loss (by P6), causing unbalanced SoC of cells in a battery pack.

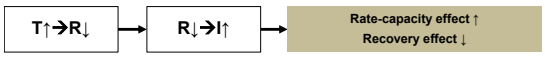

Figure 11: Uneven states of cells yield different rate-capacity/recovery effects, leading to unbalanced electrical states.

5. THE PROPOSED BATTERY THERMAL MANAGEMENT

So far, we have investigated and abstracted the physical characteristics of batteries. We have then uncovered their effects on thermal dynamics that dictate the performance of a large-scale battery system. Based on these, we now identify the thermal requirements considering the thermal dynamics, and then develop a battery thermal management policy which can satisfy the requirements based on the abstraction.

5.1 Requirements for efficient and reliable BMSes

To enhance the battery's operation-time, we need to control the physical dynamics we discussed thus far. To protect battery cells from thermal runaway (Section 4.2.1) and malfunction at low temperature (Section 4.2.2), the operation temperature (T_{cell}) should lie between its upper (T_{up}) and lower (T_{low}) bounds as follows.

R1. $T_{low} < T_{cell} < T_{up}$.

According to P3, delivering power with high temperature reduces internal resistance and improves the capacity of a battery cell during an operation cycle. Unfortunately, continuous/frequent exposure to high temperature also accelerates the degradation of battery cells during a calendar life (as shown in P4 and Section 4.2.4). According to these two characteristics, to improve capacity of cells while increasing lifetime, we should

R2'. Maximize $\left[T_{cell}(t)\right]$ for $0 < t < t_{warr} \in \mathsf{OPERATION}$, and

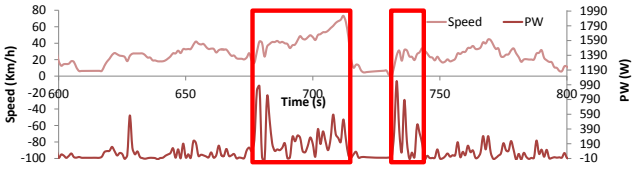

Figure 12: Driving pattern and power requirements, generated by a vehicle simulator with real driving records

R3'. Minimize $\left[\int_0^{t_{warr}} T_{cell}(t)dt | t \in \mathsf{OPERATION}\right]$,

where OPERATION is a set of time intervals in which an EV operates.

However, we cannot achieve R2' and R3' at the same time, because maximizing cell temperature will increase cumulative cell temperature. Therefore, existing studies on battery thermal management attempted to determine a static operation temperature range [24, 6], rather than dynamic thermal control, and therefore they cannot fully address the two requirements.

To achieve R2' and R3' together, we should focus on a property: EVs require power intermittently, rather than continuously. For example, requiring high power for rapid accelerations consumes most energy as shown in Fig. 12. This means, we do not have to heat cells all the time for reduction of energy dissipation, because heating the cells only during the period of high power requirement can reduce energy dissipation mostly. Therefore, separating the management period based on the power requirement can greatly reduce energy dissipation without losing potential performance improvement much. That is, we divide OPERATION into two: WORK and REST, which denote a set of time intervals in OPERATION in which a battery cell should provide a high power, and a lower power (or no power) is required, respectively; by definition, $\mathsf{OPERATION} = \mathsf{WORK} \cup \mathsf{REST}$. Then, we modify R2' and R3' such that it is possible to achieve them together by scheduling heating/cooling based on their working/resting status: maximizing working cell temperature ($T_{cell} \uparrow$, if $t \in \mathsf{WORK}$) and minimizing cumulative resting cells temperature ($T_{cell} \downarrow$, if $t \in \mathsf{REST}$), as recorded below.

R2. Maximize $\left[T_{cell}(t)\right]$ for $0 < t < t_{warr} \in \mathsf{WORK}$, and

R3. Minimize $\left[\int_0^{t_{warr}} T_{cell}(t)dt | t \in \mathsf{REST}\right]$,

Also, we should take into account issues that previous work focused on. First, we have to equalize the SoC of cells during operation-time (as mentioned in Section 4.2.5), because just one deep discharged battery cell can lead to significant reduction of capacity of the entire battery pack. Therefore, we enforce

R4. Minimize deviation $\left[\text{SoCes}\right]$.

By *rate-capacity effect*, a higher discharge rate causes inefficiency of a battery. To reduce inefficient energy loss by excessive high discharge rates, we set a discharge current limit (I_{dlim}) where the rate-capacity effect does not have much impact on the cell's capacity, and enforce cells to operate within the tolerable discharge rate range ($\leq I_{dlim}$), if possible, as follows.

R5. $I_d \leq I_{dlim}$ if possible.

Meeting R1–R5 will reduce energy dissipation and protect cells from unbalanced SoC, explosion, and malfunction. By controlling the temperature of each cell, we can directly meet R1–R3 and also alter discharge rate, addressing R4 and R5. That is, by P3 and P4, we can decrease (increase) discharge rate by lowering (raising) temperature. To realize such a control, we need a battery thermal management system and a cell-level thermal management architecture, which are detailed next.

5.2 Main thermal management: after starting a vehicle

We now propose a battery thermal management system (TMS) that meets R1–R5. Its basic principle is to heat (cool) cells to be high-discharged (rested or low-discharged). Based on each cell's SoC and the required power, our TMS determines the type of coolant for each cell to realize the principle and achieve our goal. Algorithm 1 describes how the proposed TMS operates.

5.2.1 Update states of cells (Lines 2–6)

We update all the states of battery cells in a pack to support the following steps. We can directly measure each cell's output voltage and current via sensors, and then estimate the cell's SoC, R_{int}, and V_{oc} based on the measured values [30, 20, 5, 22].

5.2.2 Set target output voltage (Lines 7–11)

This step regulates the target output voltage (V_o) based on the power requirements. Increasing V_o helps power the vehicle because the following steps heat the battery cells to reduce internal resistance in order to supply the target output voltage. Unfortunately, the power requirement may change abruptly (e.g., due to sudden acceleration or deceleration of the vehicle) and thermal control takes time. Therefore, we predict the power requirement by analyzing the driving patterns [35, 15] before segmenting the driving path for effective management in the subsequent steps.

5.2.3 Calculate the target discharge current (Line 13)

This calculates efficient discharge current (I_d) of cells for small heat dissipation and SoC balancing. As discussed in R5, we need to make each cell's discharge rate no larger than I_{dlim} for reduction of inefficient energy dissipation. Suppose $I_{dlim} \leq \frac{P_{req}}{N \cdot V_{tot}}$ holds, where P_{req} is the required power, N is the number of parallel-connected cells, and V_{tot} is the total output voltage. Then, by making each cell discharged at $\frac{I_{tot}}{N}$, we can supply the required power without excessive heat dissipation, where I_{tot} is total discharge current. To meet R4, we set I_d based on the SoC when the level of power requirement (P_{req}) is satisfied; cells with higher SoC should work more. Therefore, the discharge current (I_d) is set to $\frac{I_{tot}}{N}$ if $I_{dlim} \leq \frac{P_{req}}{N \cdot V_{tot}}$ holds, and $I_{tot}\frac{SoC}{\Sigma SoC}$ otherwise, which is recorded as:

$$I_d = \begin{cases} \frac{I_{tot}}{N}, & \text{if } I_{dlim} \leq \frac{P_{req}}{N \cdot V_{tot}}, \\ I_{tot}\frac{SoC}{\Sigma SoC}, & \text{otherwise.} \end{cases}$$

Algorithm 1 Algorithm for thermal management after starting operation

```
1: for Each module do
2:    measure V_o
3:    for Each cell X (the n-th cell) in the module do
4:       measure I_d[n] and T_cell[n];
5:       estimate SoC[n], V_oc[n] and R_int[n];
6:    end for
7:    if High power is required then
8:       increase V_o;
9:    else
10:      decrease V_o;
11:   end if
12:   for Each cell X (the n-th cell) in the module do
13:      choose efficient I_d[n];
14:      choose R_int[n] from Eq. (1);
15:      choose T_cell[n] from Eq. (3);
16:      choose T_fin[n] from Eq. (6) and thermal distribution in
         a pack;
17:      if T_fin[n] ≥ previous T_fin[n] then
18:         HeatingSet ← HeatingSet ∪ {X};
19:      else
20:         CoolingSet ← CoolingSet ∪ {X};
21:      end if
22:      if T_cell[n] ≥ T_up then
23:         CoolingSet ← CollingSet ∪ {X};
24:         HeatingSet ← HeatingSet \ {X};
25:      end if
26:   end for
27: end for
```

5.2.4 Calculate the required thermal fins' temperature (Lines 14–16)

After setting I_d and V_o, we can calculate the required R_{int} and T_{cell} from Eqs. (1) and (3) as:

$$c_3 T_{cell}^3 + c_2 T_{cell}^2 + c_1 T_{cell} + c_0 = R_{int} = \frac{V_{oc} - V_o}{I_d},$$

while Eq. (6) calculates the desirable ambient temperature (T_{amb}).

Cell temperature depends on ambient temperature including the temperature of thermal fins, and the ambient temperature can be estimated by updating temperature distribution in a battery pack as shown in Fig. 13. Note that the temperature distribution can be calculated based on temperatures measured by sensors in a

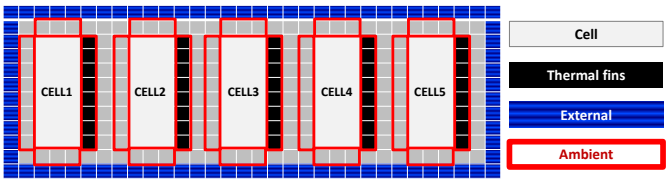

Figure 13: Temperature distribution and ambient temperature of cells in a battery pack

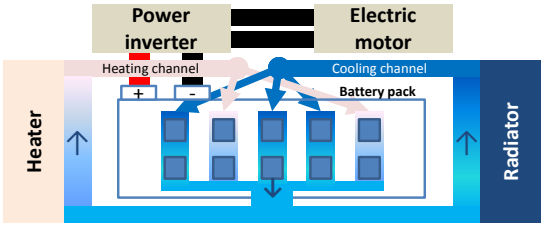

Figure 14: Thermal management for battery packs

pack. Based on the temperature distribution, we can obtain thermal fins' temperatures that achieve the target ambient temperature.

5.2.5 *Select the coolant type for thermal fins (Lines 17–25)*

Lines 17–21 determine the coolant type (heated or cooled) for cells based on current and required fin temperatures. In Lines 22–25, we choose the cells whose temperature is higher than the upper limit, and move them from HeatingSet to maintain thermal stability.

As discussed earlier, the way of calculating I_d addresses R4 and R5. Then, all the steps will meet R2 and R3, since cells are heated (cooled) when they need high power (otherwise). The final step (Lines 22–25) guarantees R1. So, Algorithm 1 meets R1–R5.

5.3 Thermal Management Architecture

R1–R3 can be met by the existing thermal architecture, since it can regulate the temperature of battery cells in a timely manner. To satisfy R4 and R5, we need a new architecture which can cool/heat each cell selectively as shown in Fig. 14. The new architecture is not much different from existing architectures. While existing BMSes are already been equipped with the heating/cooling capability (e.g., [10, 9]), we need to add more coolant flow valves between the heating/cooling channel and thermal fins for each cell, as shown in the figure. Each coolant control valve should be able to select the type (either heating or cooling) of coolant for cells.

6. EVALUATION

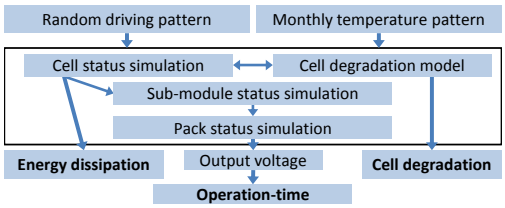

Figure 15: Evaluation tools

We now evaluate the performance improvement by the proposed TMS, focusing on whether or not the goal stated in Section 3 is met. We first introduce the performance metrics and evaluation tools/settings to be used. We then present the evaluation results, and finally make remarks on the TMS implementation.

6.1 Evaluation metrics

To evaluate the performance of the proposed TMS, we conducted various simulations, and recorded relevant internal battery states. To check if the goal is achieved or not, we extracted the information of battery operation-time. Also, for the analysis of the simulation results, we use (i) *energy dissipation* to show how fast battery energy is depleted, and (ii) *internal resistance* to assess the degradation rate of batteries.

6.2 Evaluation tools and settings

To study battery behavior under the proposed TMS, we designed a comprehensive simulator which can calculate each cell's internal states under realistic situations. Also, to obtain realistic thermal stress values for each cell, we selected three US cities representing cold, medium, and hot regions: Anchorage, AK; Ann Arbor, MI; and Phoenix, AZ, denoted by AC, AA and PH, respectively. Fig. 15 provides an overview, components of which are described next.

6.2.1 *Dualfoil5 (cell-level battery simulator)*

Dualfoil5 is a popular battery simulator written in Fortran, and can simulate various types of batteries including the lithium-metal, lithium-ion, and sodium-ion batteries [7]. The program reads the load profile as a sequence of constant current steps, and the battery lifetime is obtained from the output by reading off the time at which the cell potential drops below the cutoff voltage. The equations and methods used in the program rely on an electrochemical model that describes the charge and discharge of a lithium ion battery developed by Marc Doyle *et al.* [7].

6.2.2 *CarSim with driving patterns (power requirement)*

To acquire realistic power requirements, we exploit US driving patterns [32], a daily driving pattern model [31, 21], and CarSim [25]. CarSim is a well-known and

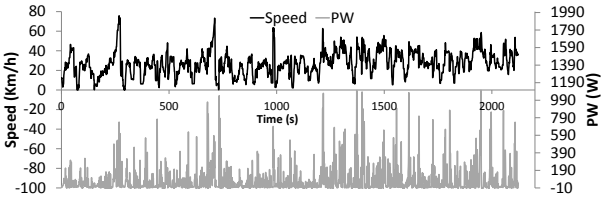

Figure 16: Speed and power requirement profiles

widely-used vehicle modeling tool, simulating the dynamic behavior of vehicles under specified driving conditions, and calculating the required power during driving. We obtain the power requirement profile as follows. First, a daily driving pattern model with a set of US real driving patterns yields daily driving patterns. These daily driving patterns are then fed to CarSim to generate the power requirement. Fig. 16 shows a set of speed and power requirement profiles generated by this process.

6.3 Evaluation results

We evaluate the following three thermal management schemes:

- BASE: no thermal management;
- EX: existing approaches described in Section 2 (pack-level cooling/heating only for thermal stability); and
- MSC: our thermal management described in Section 5 (active cell-level cooling/heating for efficient BMSes).

For these evaluations, we generated realistic driving and external temperature profiles before simulating the behavior of a battery system with the above three schemes. The three metrics described in Section 6.1 are then extracted from the simulation results.

6.3.1 Operation-times after one-year operation

We ran simulation and extracted operation-times of each scheme under various stress conditions. Average operation-times are then calculated to show the overall performance of each scheme. Table 1 shows the ratio of the average operation-time of MSC (and EX), to that of BASE. As shown in the table, MSC improves the operation-time by up to 204% and 58.4%, respectively over BASE and EX. Also, MSC keeps all the batteries within a tolerable temperature range to prevent explosion or malfunction as shown in Fig. 17; in AC, some batteries operate at extremely cold temperature under BASE, potentially leading to malfunction or inefficient usage of the battery pack, whereas all the cells in a pack operate within a tolerable temperature range under MSC and EX.

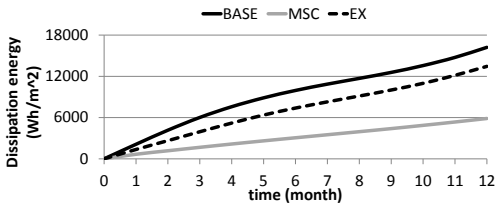

Figure 18: Cumulative energy dissipation for one-year operation in AA

	Average ℓ_{op} (Sec)		
City, Month	AC	AA	PH
EX/BASE	1.92	0.92	1.03
MSC/BASE	3.04	1.40	1.62

Table 1: Average operation-time

From Table 1, we can observe that MSC's improvement in AC is more pronounced than that in AA and PH, because there is more room for performance improvement in colder areas, which we will elaborate in Section 6.3.2. As shown in Table 1, MSC effectively exploits such room for improvement. For a more detailed analysis for the improvement of MSC, we investigate energy dissipation and performance degradation in the following subsections.

6.3.2 Energy dissipation

Our TMS in Section 5 includes several methods to decrease energy dissipation. They actually contribute to the extension of operation-time, since reducing energy dissipation increases available energy in the cells, which, in turn, extends the operation-time.

We compare the energy dissipation of the three thermal management schemes when the car operates in AC, AA and PH. Table 2 shows energy dissipation when drivers operate their cars repeating the same driving pattern every day for a year. Fig. 18 shows an example energy dissipation of each management scheme. Compared to BASE, MSC reduces energy dissipation by 70.6% in AC, 63.8% in AA, and 48.4% in PH. MSC is even better than EX in that it can reduce more energy dissipation by up to 58.6% than EX. This reduction of energy dissipation extends the operation-time under MSC.

	Cumulative energy dissipation (Wh/m^2)		
City	AC	AA	PH
BASE	20978	16216	10474
EX	14910	13450	9976.5
MSC	6167.5	5864.6	5403.5

Table 2: Energy dissipation after one year of operation

An interesting point to note is that the difference between energy dissipation of MSC (or EX) and that of BASE is significant in AC. This can be reasoned as fol-

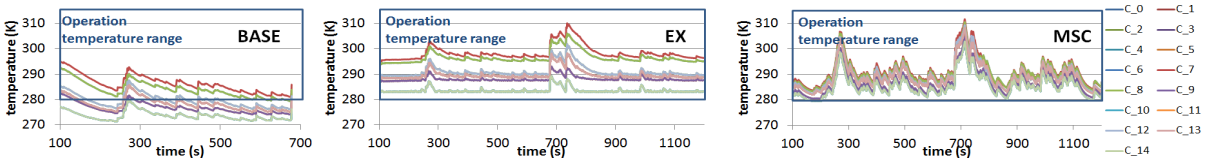

Figure 17: Example of thermal management in AC; C_x means Cell x

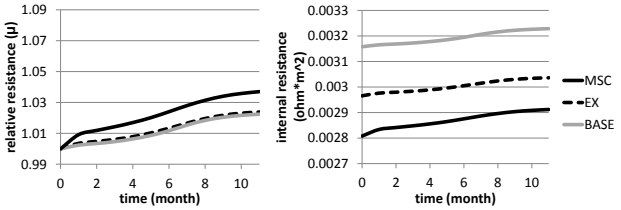

Figure 19: Relative resistance and internal resistance in AA

lows. In a hotter area, the efficiency is higher (or smaller energy dissipation) even without any thermal management (i.e., BASE), because high temperature increases the chemical reaction rate in a battery. So, in AC where temperature is extremely low in winter, MSC and EX heat the cells to attain effective operation temperature; we observe from Fig. 17 that EX and MSC yield a tolerable temperature range for battery cells. This reduces energy dissipation.

MSC reduces energy dissipation significantly more than EX, since it not only timely cools/heats the cells in order to reduce energy dissipation, but also selectively cools/heats the cells for SoC equalization. Therefore, each cell operates more efficiently under MSC, by reducing temperature differences between cells. The reduction of energy dissipation is one of the dominant reasons for improving the operation-time.

6.3.3 *Degradation of battery performance*

The degree of battery performance degradation depends on its cumulative exposure to high temperature. To evaluate the performance degradation, we compare cells' degradation levels, which are represented by relative resistance and the absolute value of internal resistance, under each thermal management scheme in AC, AA and PH during a 1-year period. Of these three locations, we chose AA, since the results for other locations exhibit a similar or same trend.

Figs. 19(a) and (b) plot relative resistance and the absolute value of internal resistance, respectively. As shown in Fig. 19(a), MSC leads to a little bit faster degradation than the other schemes, because MSC actively cools/heats each cell. However, such active control reduces the absolute value of internal resistance; as shown in Fig. 19(b), internal resistance after one-year usage under MSC is smaller than that under other schemes. This implies that MSC, despite higher relative resistance, is still more efficient for up to one year. These results validate an increase of operation-time discussed in Section 6.3.1, i.e., MSC is efficient in using a battery pack.

6.4 Remarks on implementation

We can build the TMS based on the existing approaches for cooling and heating engines and batteries in the current vehicles on the market. To implement the BMS that accommodates the proposed TMS, some additional hardware should be installed in each battery pack. Measuring the output voltage and discharge current of cells requires sensors, just as other BMSes [13, 19, 11] do. Additional control flow valves are also required for cell-level thermal controls; their performance and reliability should be considered since they directly affect the effectiveness of battery management. It would be interesting to design a BMS with efficient and reliable management of hardware sensors and actuators by considering their physical characteristics along with battery dynamics. This is part of our future work.

7. CONCLUSION

To resolve increasing demand to make EVs less expensive and safer, BMSes should cope with thermal and general issues that affect efficiency and reliability of BMSes. A thermal management is the key to addressing these issues, since temperature has significant impact on electrical states of BMSes. In this paper, we presented how to achieve efficient and reliable BMSes using thermal controls. We proposed a battery thermal management scheme that cools/heats battery cells timely and selectively based on the analysis for impacts of power requirements and temperature variation on electrical states of battery cells. To support this scheme, we also proposed thermal management architecture, which is able to cool/heat battery cells selectively. Our evaluation with realistic simulation showed that our approach makes a significant improvement in BMSes' efficiency without compromising their reliability, over a simple method often seen in the existing BMSes.

It would be interesting to explore ways of improving thermal management based on the proposed architecture. We may be able to improve performance with a

more accurate and adaptive abstraction model instead of the basic model used in this paper. We can also improve the BMS efficiency by heating/cooling cells in advance with more accurate power requirement prediction [35, 15].

Acknowledgement

The work reported in this paper was supported in part by the NSF under grants CNS-1138200 and CNS-1329702.

8. REFERENCES

[1] T. M. Bandhauer, S. Garimella, and T. F. Fuller. A critical review of thermal issues in lithium-ion batteries. *Journal of The Electrochemical Society*, 2011.

[2] L. Benini, A. Macii, E. Macii, M. Poncino, and R. Scarsi. Scheduling battery usage in mobile systems. *IEEE Transactions on VLSI systems*, 11(6):1136–1143, 2003.

[3] D. Bernardi, E. Pawlikowski, and J. Newman. A general energy balance for battery systems. *Journal of the electrochemical society*, 132:5–12, 1985.

[4] Y. Chen, L. Song, and J. Evans. Modeling studies on battery thermal behaviour, thermal runaway, thermal management, and energy efficiency. In *Proceedings of Energy Conversion Engineering Conference, the 31st Intersociety*, volume 2, pages 1465–1470 vol.2, 1996.

[5] Y.-H. Chiang, W.-Y. Sean, and J.-C. Ke. Online estimation of internal resistance and open-circuit voltage of lithium-ion batteries in electric vehicles. *Journal of Power Sources*, 196(8):3921 – 3932, 2011.

[6] W. J. Culver. High-value energy storage for the grid: A multi-dimensional look. *The Electricity Journal*, 23(10):59–71, 2010.

[7] M. Doyle and J. Newman. Dualfoil5. `http://www.cchem.berkeley.edu/jsngrp/fortran.html`.

[8] O. Erdinc, B. Vural, and M. Uzunoglu. A dynamic lithium-ion battery model considering the effects of temperature and capacity fading. In *Clean Electrical Power, 2009 International Conference on*, pages 383–386, 2009.

[9] FordMotorCompany. Ford uses innovative liquid-cooled battery system to help focus electric owners maximize range. `http://www.at.ford.com/news/cn/Pages/FordUsesInnovativeLiquidCooledBatterySystemtoHelpFocus\ElectricOwnersMaximizeRange.aspx`, 2013.

[10] GeneralMotors. The chevrolet volt cooling/heating systems explained. `http://gm-volt.com/2010/12/09/the-chevrolet-volt\-coolingheating-systems-explained/`, 2009.

[11] L. He, L. Gu, L. Kong, Y. Gu, C. Liu, and T. He. Exploring adaptive reconfiguration to optimize energy efficiency in large battery systems. In *Proceedings of the 34th IEEE Real-Time Systems Symposium*, 2013.

[12] M. Jongerden, B. Haverkort, H. Bohnenkamp, and J. Katoen. Maximizing system lifetime by battery scheduling. In *Dependable Systems Networks, 2009. IEEE/IFIP International Conference on*, pages 63–72, 2009.

[13] R. Kaiser. Optimized battery-management system to improve storage lifetime in renewable energy systems. *Journal of Power Sources*, 168(1):58–65, 2007.

[14] H. Kiehne. *Battery Technology Handbook*. CRC Press, second edition, 2003.

[15] E. Kim, J. Lee, and K. G. Shin. Real-time prediction of battery power requirements for electric vehicles. In *Proceedings the 4th ACM/IEEE International Conference on Cyber-Physical Systems*, Philadelphia, PA, Apr 2013.

[16] G.-H. Kim and A. Pesaran. Battery thermal management system design modeling. In *the 22nd International Battery, Hybrid and Fuel Cell Electric Vehicle Conference and Exhibition*, Yokohama, Japan, Oct 2006.

[17] H. Kim and K. G. Shin. On dynamic reconfiguration of a large-scale battery system. In *Proceedings of the 15th IEEE Real-Time and Embedded Technology and Applications Symposium*, pages 87–96, 2009.

[18] H. Kim and K. G. Shin. Scheduling of battery charge, discharge, and rest. In *Proceedings of the 30th IEEE Real-Time Systems Symposium*, pages 13–22, 2009.

[19] H. Kim and K. G. Shin. Dependable, efficient, scalable architecture for management of large-scale batteries. In *Proceedings of the 1st ACM/IEEE International Conference on Cyber-Physical Systems*, pages 178–187, 2010.

[20] S. Lee, J. Kim, J. Lee, and B. Cho. State-of-charge and capacity estimation of lithium-ion battery using a new open-circuit voltage versus state-of-charge. *Journal of Power Sources*, 185(2):1367 – 1373, 2008.

[21] T.-K. Lee, B. Adornato, and Z. Filipi. Synthesis of real-world driving cycles and their use for estimating phev energy consumption and charging opportunities: Case study for midwest/u.s. *Vehicular Technology, IEEE Transactions on*, 60(9):4153–4163, 2011.

[22] Y. Li, R. Anderson, J. Song, A. Phillips, and X. Wang. A nonlinear adaptive observer approach for state of charge estimation of lithium-ion batteries. In *Proceedings of American Control Conference, 2011*, pages 370–375, 2011.

[23] D. Linden and T. Reddy. *Handbook of batteries*. McGraw-Hill, third edition, 2002.

[24] A. A. P. Matthew Zolot and M. Mihalic. Thermal evaluation of toyota prius battery pack. In *SAE Technical Paper 2002-01-1962*, 2002.

[25] MechanicalSimulationCorporation. Carsim simulator. `http://www.carsim.com/products/carsim/index.php`. [Online; accessed 21-October-2012].

[26] Merriam-Webster. `http://www.merriam-webster.com/`.

[27] C. Park and A. Jaura. Dynamic thermal model of li-ion battery for predictive behavior in hybrid and fuel cell vehicles. In *SAE Technical Paper 2003-01-2286*, 2003.

[28] A. Pesaran. Battery thermal management in evs and hevs: Issues and solutions. In *the 4th Vehicle Thermal Management Systems Conference and Exhibition*, Las vegas, Nevada, Feb 2001.

[29] A. Pesaran, S. Burch, and M. Keyser. An approach for designing thermal management systems for electric and hybrid vehicle battery packs. In *the 4th Vehicle Thermal Management Systems Conference and Exhibition*, London, UK, May 1999.

[30] G. L. Plett. Extended kalman filtering for battery management systems of lipb-based hev battery packs: Part 3. state and parameter estimation. *Journal of Power Sources*, 134(2):277 – 292, 2004.

[31] R. Smith, S. Shahidinejad, D. Blair, and E. Bibeau. Characterization of urban commuter driving profiles to optimize battery size in light-duty plug-in electric vehicles. *Transportation Research Part D: Transport and Environment*, 16(3):218–224, 2011.

[32] TheNewNextGenerationSimulationCommunity. Introduction of NGSIM. `http://ngsim-community.org`. [Online; accessed 21-October-2012].

[33] E. Thomas, I. Bloom, J. Christophersen, and V. Battaglia. Statistical methodology for predicting the life of lithium-ion cells via accelerated degradation testing. *Journal of Power Sources*, 184(1):312–317, 2008.

[34] E. Thomas, I. Bloom, J. Christophersen, and V. Battaglia. Rate-based degradation modeling of lithium-ion cells. *Journal of Power Sources*, 206(0):378–382, 2012.

[35] H. Yu, F. Tseng, and R. McGee. Driving pattern identification for ev range estimation. In *Electric Vehicle Conference, 2012 IEEE International*, pages 1–7, 2012.